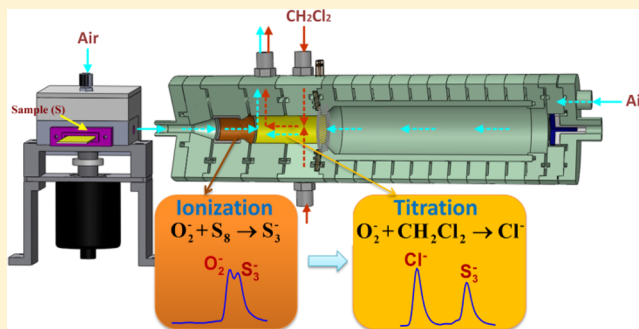


## Sensitive Detection of Black Powder by a Stand-Alone Ion Mobility Spectrometer with an Embedded Titration Region

Xixi Liang,<sup>†,‡</sup> Qinghua Zhou,<sup>†,‡</sup> Weiguo Wang,<sup>†</sup> Xin Wang,<sup>†</sup> Wendong Chen,<sup>†,‡</sup> Chuang Chen,<sup>†,‡</sup> Yang Li,<sup>†</sup> Keyong Hou,<sup>†</sup> Jinghua Li,<sup>†</sup> and Haiyang Li<sup>\*,†</sup><sup>†</sup>Dalian Institute of Chemical Physics, Chinese Academy of Sciences, Dalian, 116023, People's Republic of China<sup>‡</sup>Graduate University of Chinese Academy of Sciences, Beijing, 100039, People's Republic of China

## S Supporting Information

**ABSTRACT:** Sensitive detection of black powder (BP) by stand-alone ion mobility spectrometry (IMS) is full of challenges. In conventional air-based IMS, overlap between the reactant ion  $\text{O}_2^-(\text{H}_2\text{O})_n$  peak and the sulfur ion peak occurs severely; and common doping methods, providing alternative reactant ion  $\text{Cl}^-(\text{H}_2\text{O})_n$ , would hinder the formation of ionic sulfur allotropes. In this work, an ion mobility spectrometer embedded with a titration region (TR-IMS) downstream from the ionization region was developed for selective and sensitive detection of sulfur in BP with  $\text{CH}_2\text{Cl}_2$  as the titration reagent. Sulfur ions were produced via reactions between sulfur molecules and  $\text{O}_2^-(\text{H}_2\text{O})_n$  ions in the ionization region, and the remaining  $\text{O}_2^-(\text{H}_2\text{O})_n$  ions that entered the titration region were converted to  $\text{Cl}^-(\text{H}_2\text{O})_n$  ions, which avoided the peak overlap as well as the negative effect of  $\text{CH}_2\text{Cl}_2$  on sulfur ions. The limit of detection for sulfur was measured to be 5 pg. Furthermore, it was demonstrated that this TR-IMS was qualified for detecting less than 5 ng of BP and other nitro-organic explosives.



Black powder (BP) is an explosive mixture, consisting of sulfur, charcoal, and potassium nitrate, with a typical weight ratio of about 1:1.5:7.5.<sup>1,2</sup> Owing to its unrestricted availability, low-cost, flammability, and explosive properties, BP was one of the most common explosive fillers in criminal and terrorist attacks, accounting for 33.2% of injuries and 27.1% of deaths in bombings together with smokeless powder in the United States.<sup>3</sup> Therefore, field-deployable detection techniques for trace amounts of BP are in high demand for civilian security.

With the advantages of low detection limits, fast response, and portability, ion mobility spectrometry (IMS) has been one of the most favorable technologies in trace detection of nitro-organic explosives, such as trinitrotoluene (TNT), pentaerythritol tetranitrate (PETN), cyclotrimethylenetrinitramine (RDX), etc.<sup>4–6</sup> However, rare investigations on detection of BP with IMS have been reported. Fetterholf et al. attempted to detect BP by a commercial IMS (IONSCAN 2000) using hexachloroethane mixed air as the carrier gas, but no product ions peak was observed.<sup>7</sup> McGann et al. reported the observation of product ions for BP using IonTrack IMS;<sup>8</sup> nevertheless, they gave neither the spectrum nor the limit of detection. Recently, Hill et al. observed a broad product ion peak for BP with nitrogen as the carrier and the reactant gas via an ion mobility/time-of-flight mass spectrometer, a homemade stand-alone IMS, and a commercial ion trap mobility spectrometer. Also they assigned the product ions with an

average reduced mobility value of  $2.28 \text{ cm}^2 \text{ V}^{-1} \text{ s}^{-1}$  to  $\text{S}_n^-$  ( $n = 1–5$ ).<sup>9</sup> However, the amounts of BP used in that work were as large as 5–10 mg, and the sensitivity and linear range was not studied.

Whereas, it still seems to be full of challenges to sensitively detect BP by stand-alone IMS with air as the carrier and drift gas. First, the peak of BP product ions is severely overlapped with that of reactant ions  $\text{O}_2^-(\text{H}_2\text{O})_n$  (seen in Figure 2a). Thus, it is tough to distinguish a weak product signal from the tail of the strong reactant ion peak, especially for trace BP samples. A potential method to change the peak position of the remaining  $\text{O}_2^-(\text{H}_2\text{O})_n$  is adding dopant such as chlorohydrocarbon, which was often used to enhance the detection of nitro-organic explosives.<sup>10,11</sup> However, when the reactant ion is converted to  $\text{Cl}^-(\text{H}_2\text{O})_n$ , sulfur ions for BP could not be formed since the electron affinity (EA) of sulfur ( $\text{EA}(\text{S}_8) = 3.590 \text{ eV}^{12}$ ) is smaller than that of chlorine ( $\text{EA}(\text{Cl}) = 3.613 \text{ eV}^{12}$ ).

Therefore, in this work, we introduce a special stand-alone ion mobility spectrometer embedded with a titration region (TR-IMS) to inhibit the peak overlap in BP detection. The titration region was designed to follow the ionization region for annihilating the remaining reactant ions  $\text{O}_2^-(\text{H}_2\text{O})_n$  with dichloromethane as the titration reagent, allowing for improved

Received: February 9, 2013

Accepted: April 26, 2013

Published: April 26, 2013

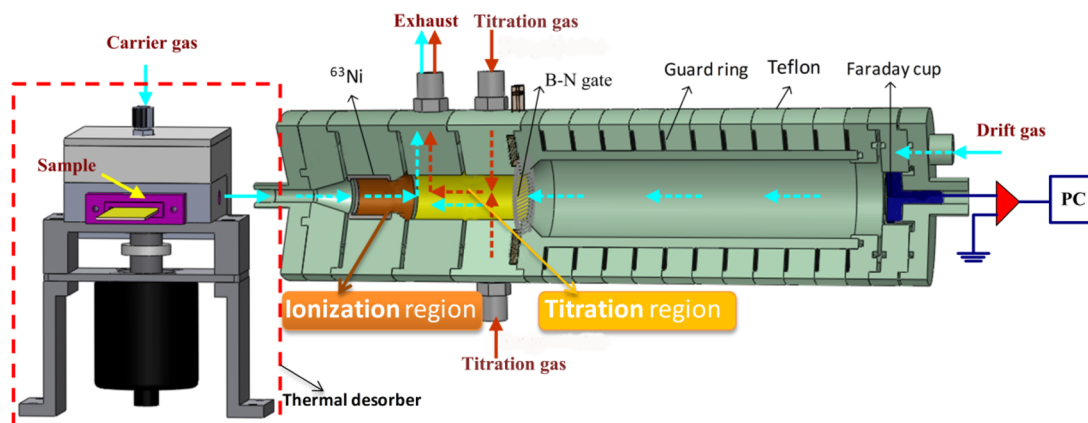


Figure 1. Schematic experimental setup of the newly designed ion mobility spectrometer embedded with a titration region (TR-IMS).

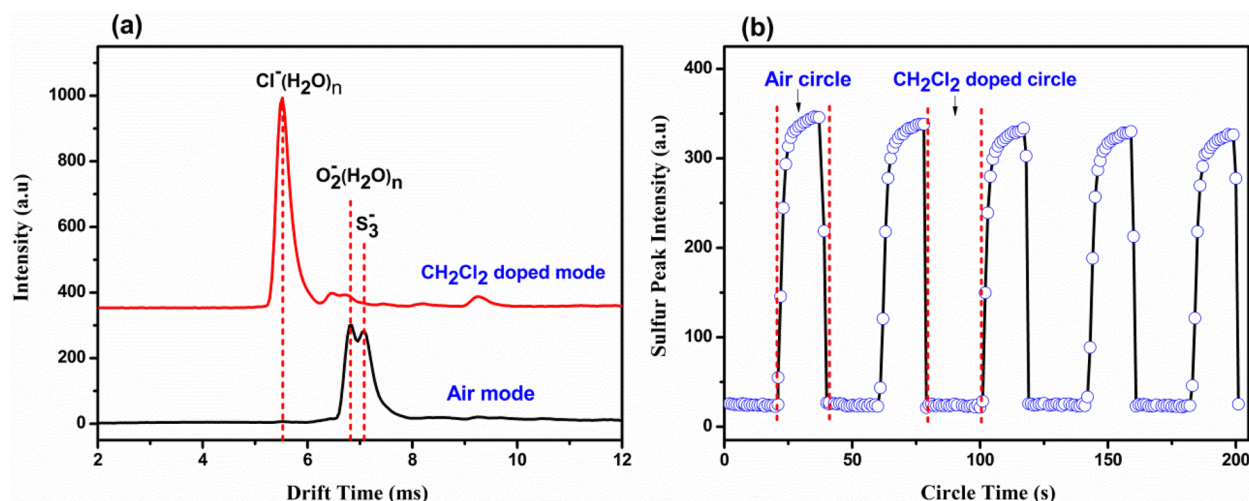


Figure 2. (a) IMS spectra obtained by the modified system for 100 pg of sulfur using  $\text{CH}_2\text{Cl}_2$  doped air and pure air as the carrier gas, respectively. (b) Time-dependent profiles of sulfur peak intensity for consecutively detecting 50 ng of sulfur in a periodic switch of these two carrier gas modes. Each circle time for these two modes was 20 s.

resolution and better sensitivity of the BP product ion. Finally, the performances of TR-IMS apparatus on common military explosives were also implemented.

## EXPERIMENTAL SECTION

A TR-IMS was constructed in our laboratory, schematically displayed in Figure 1. Compared with the conventional IMS, a titration region (14 mm i.d. and 16 mm length) was added, which was located between the ionization region (14 mm i.d. and 24 mm length) and the Bradbury–Nielson (BN) gate. Used as the titration reagent, 20 ppm  $\text{CH}_2\text{Cl}_2$  was introduced into the titration region from the inlet ports near the BN gate and reacted with the remaining  $\text{O}_2^-(\text{H}_2\text{O})_n$  ions, then flowed out the titration region from the outlet port near the ionization region. Thus, the remaining  $\text{O}_2^-(\text{H}_2\text{O})_n$  ions was converted to  $\text{Cl}^-(\text{H}_2\text{O})_n$  ions to avoid the peak overlap. At the same time, most  $\text{CH}_2\text{Cl}_2$  could not enter the ionization source avoiding the negative effect of  $\text{CH}_2\text{Cl}_2$  on the formation of sulfur ions. Then, these ions were injected into the drift region through the BN gate with an injection pulse of 200  $\mu\text{s}$  and were collected by a Faraday plate.

The purified air was used as the carrier gas, titration gas, and drift gas with flow rates of 200, 200, and 600 mL/min, respectively, which was filtrated by silica gel, activated carbon,

and 13 X molecular sieves to reduce the air moisture to be below 1 ppm monitored by a dew point sensor (DP300, CS Instrument GMH). A homemade thermal desorber was used for sample introduction. The operating parameters and the introduction of chemicals were shown in the Supporting Information.

## RESULTS AND DISCUSSION

With purified air as the carrier gas, as shown in Figure 2a, severe peak overlap between the reactant ions  $\text{O}_2^-(\text{H}_2\text{O})_n$  and sulfur ions were observed, which was obtained via a modified IMS instrument (as shown in Figure S-1 in the Supporting Information). When the carrier gas was doped with 20 ppm dichloromethane, no evident signal for sulfur could be found. Furthermore, by periodically switching the carrier gas between purified air and  $\text{CH}_2\text{Cl}_2$  doped air, the intensity of sulfur signal exhibited the “on-off” temporal profile as shown in Figure 2b. It is clear that the intensity of sulfur was reduced from 350 mV to 20 mV when  $\text{CH}_2\text{Cl}_2$  was doped in the carrier gas, which indicated that the predominated ion  $\text{Cl}^-(\text{H}_2\text{O})_n$  seriously hindered the formation of ionic sulfur allotropes. Moreover, a conventional IMS was used to detect 100 pg of sulfur by doping the carrier gas with 2.5–21.5 ppm  $\text{CH}_2\text{Cl}_2$ , and the results also indicated that the conventional doping method was not

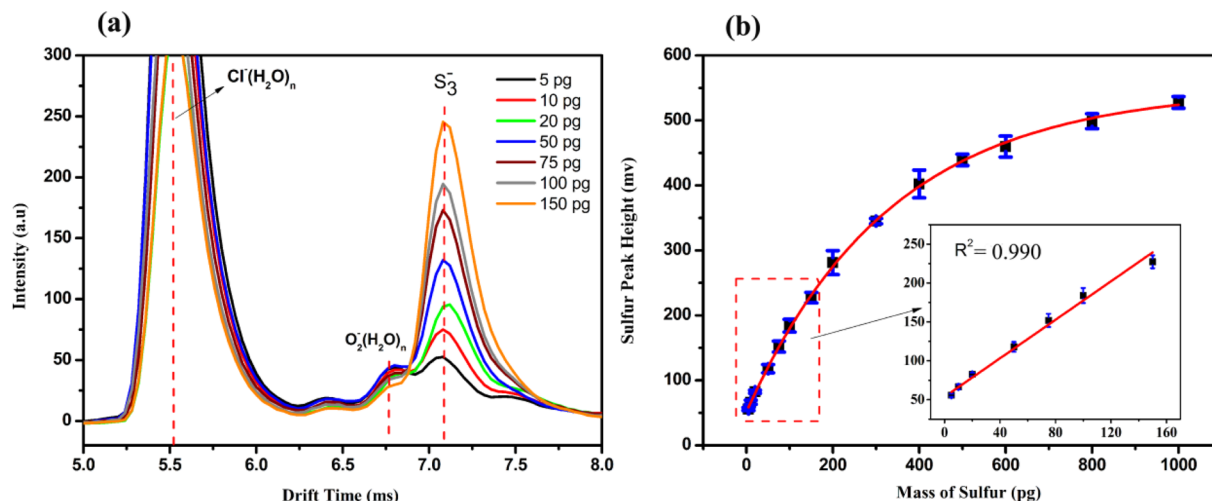


**Figure 3.** (a) TR-IMS spectra of 5–150 pg of sulfur with 20 ppm  $\text{CH}_2\text{Cl}_2$  as the titration reagent. (b) Response curve and linear calibration curve (insert plot) for sulfur.

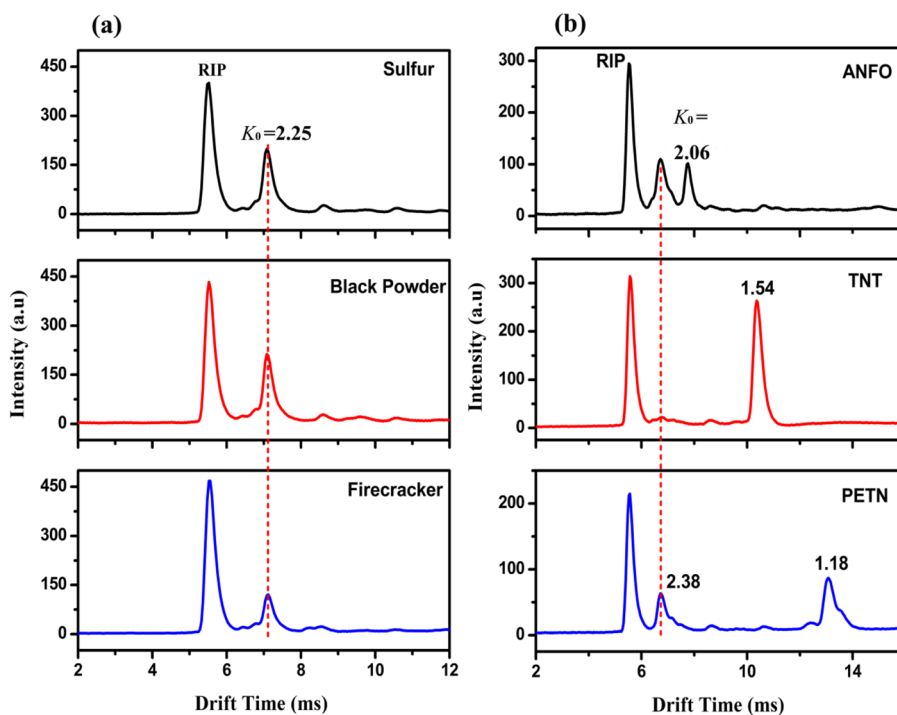


**Figure 4.** (a) TR-IMS spectra for 100 pg of sulfur, 5 ng of black powder, and 5 ng of firecracker. (b) TR-IMS spectra for 5 ng of ANFO, 5 ng of TNT, and 5 ng of PETN.

impracticable, which was discussed in detail in the Supporting Information (Figure S-2).

In TR-IMS, with 20 ppm  $\text{CH}_2\text{Cl}_2$  as the titration reagent, we detected 5–150 pg sulfur samples and their ion mobility spectra are depicted in Figure 3a. It is obvious that most of the remaining  $\text{O}_2^-(\text{H}_2\text{O})_n$  ions (at 6.86 ms) were efficiently converted to  $\text{Cl}^-(\text{H}_2\text{O})_n$  ions (at 5.52 ms) with the conversion proportion around 92%, while the sulfur peak persisted at 7.08 ms ( $K_0 = 2.25 \text{ cm}^2 \text{ V}^{-1} \text{ s}^{-1}$ ). Indeed, down to 5 pg of sulfur could be sensitively identified by the TR-IMS; in this case, the intensity of sulfur peak was 55 mV, still higher than that of the residual  $\text{O}_2^-(\text{H}_2\text{O})_n$  peak about 45 mV. In Figure 3a, it is also clear that the intensity of the sulfur peak was increased with the increasing amount of sulfur. Plotting the intensity of the sulfur peak versus the amount of sulfur from 5 to 1000 pg, as shown

in Figure 3b, it was found that the linear response range for sulfur was from 5 to 150 pg with a correlation coefficient  $R^2$  of 0.990, illustrated in the insert curve. Meanwhile, the repeatability was found to be satisfactory for the measurement of sulfur by TR-IMS, with the average relative standard deviation (RSD) of 3.8% for five measurements. In addition, regardless of the presence of dichloromethane, the drift time of sulfur peak in Figure 3a is the same as that in Figure 2a, indicating that the titration reagent did not affect the sulfur ions formed in the ionization region. The peak to peak resolution between  $\text{Cl}^-(\text{H}_2\text{O})_n$  peak and sulfur peak was calculated to be 3.06 according the previous equation,<sup>13</sup> which was 6 times higher than that between the  $\text{O}_2^-(\text{H}_2\text{O})_n$  peak and sulfur peak in Figure 2a, indicating that the complete baseline separation was achieved.



The negative product ions of sulfur in  $^{63}\text{Ni}$  ion source were identified by a homemade ion trap mass spectrometer (ITMS). As shown in Figure S-3 in the Supporting Information, there are three ion species of  $m/z$  96,  $m/z$  98, and  $m/z$  128 with relative abundances of 100%, 13.3%, and 2.7%, respectively. The ions at  $m/z$  = 96 and 98 were attributed to  $\text{S}_3^-$ , as their intensity ratio of 7.5 perfectly matched the theoretical isotopic ratio of  $^{32}\text{S}_3^-$  ( $m/z$  = 96) and  $^{32}\text{S}_2^{34}\text{S}_1^-$  ( $m/z$  = 98). The weakest peak at  $m/z$  = 128 was assigned to allotropes of  $\text{S}_4^-$ . This result is in good agreement with the previous experiments,<sup>9,14</sup> where the  $\text{S}_3^-$  was also the dominant negative ion.

The  $\text{S}_3^-$  and  $\text{S}_4^-$  ions may be formed through electron-transfer reaction between  $\text{O}_2^-(\text{H}_2\text{O})_n$  and gaseous  $\text{S}_8$  (reactions 1 and 2) in the ionization region. It might involve complicated reactions such as a ring-opening polymerization of the  $\text{S}_8$  rings and freely rotating chains to obtain the final product ions.<sup>15,16</sup> It was deduced that the remaining  $\text{O}_2^-(\text{H}_2\text{O})_n$  ions were converted to  $\text{Cl}^-(\text{H}_2\text{O})_n$  in the titration region through reaction 3 according to the negative Gibbs energy  $\Delta_r G$  of reaction 3. Also, the positive  $\Delta_r G$  of reactions between  $\text{CH}_2\text{Cl}_2$  and  $\text{S}_3^-/\text{S}_4^-$  indicated that these reactions are prohibited in thermodynamics. The detailed calculation processes can be found in the Supporting Information.



The ability of TR-IMS to detect black powder, firecrackers, and other explosives are demonstrated in Figure 4a,b. As depicted in Figure 4a, the TR-IMS spectra of 5 ng of BP and 5 ng of firecracker show the same characteristic peak centered at 7.08 ms as sulfur, indicating that the same product ions of  $\text{S}_3^-/\text{S}_4^-$  were formed. The theoretical amount of sulfur in 5 ng of standard black powder (containing 10% wt of sulfur<sup>1</sup>) was calculated to be about 500 pg; however, the intensity for 5 ng of BP was just about 200 mV, which was corresponding to only 100 pg of sulfur, suggesting that only  $1/5$  of the sulfur in BP could be vaporized to the gaseous phase in the thermal desorber. The incomplete desorption is probably ascribed to that the sulfur in BP is partly adsorbed by the charcoal (15% wt of BP<sup>1</sup>). Figure 4b shows the TR-IMS spectra of 5 ng of ammonium nitrate/fuel oil (ANFO), 5 ng of TNT, and 5 ng of PETN. The peak heights of the product ions of these explosives varied from 70 mV to 250 mV, which means that the TR-IMS is completely qualified for tracing common military explosives.

The characteristic product ions for BP, ANFO, TNT, and PETN with reduced mobility of 2.25, 2.06, 1.54, and  $1.18 \text{ cm}^2 \text{ V}^{-1} \text{ s}^{-1}$  are assigned to  $\text{S}_3^-/\text{S}_4^-$ ,  $[\text{HNO}_3 \cdot \text{NO}_3]^-$ ,  $[\text{TNT} - \text{H}]^-$ , and  $[\text{PETN} \cdot \text{NO}_3]^-$ , respectively, as shown in Figure S-4 in the Supporting Information, which well agrees with the literature,<sup>9,17,18</sup> and suggests that the titration reagent does not affect the reactions in the ionization region somehow. Meanwhile, the peaks at 6.70 ms with  $K_0 = 2.38 \text{ cm}^2 \text{ V}^{-1} \text{ s}^{-1}$  appeared in ANFO and PETN and were tentatively considered as  $\text{NO}_3^-$  according to the previous literature.<sup>17</sup>

## CONCLUSIONS

In this work, a new air-based ion mobility spectrometer embedded with a titration region was constructed for efficient detection of black powder. The novel design of TR-IMS was to make the ionization of sulfur and the depletion of hydrated

oxygen ions take place in different regions of the spectrometer. Using dichloromethane as the titration reagent, the remaining reactant ions  $\text{O}_2^-(\text{H}_2\text{O})_n$  were converted to  $\text{Cl}^-(\text{H}_2\text{O})_n$  ions in the titration region, successfully avoiding the severe peak overlap between the  $\text{O}_2^-(\text{H}_2\text{O})_n$  and sulfur ions. Also, the negative effect of  $\text{CH}_2\text{Cl}_2$  on the reaction of sulfur with  $\text{O}_2^-(\text{H}_2\text{O})_n$  ions could be avoided by preventing  $\text{CH}_2\text{Cl}_2$  from entering the ionization source. Therefore, the TR-IMS exhibited an excellent performance on the detection of sulfur at the picogram level and the limit of detection for black powder was less than 5 ng. Finally, the capability of TR-IMS for detection of other military explosives such as ANFO, TNT, and PETN at the nanogram level were well demonstrated.

## ASSOCIATED CONTENT

### Supporting Information

Additional information as noted in text. This material is available free of charge via the Internet at <http://pubs.acs.org>.

## AUTHOR INFORMATION

### Corresponding Author

\*E-mail: [hli@dicp.ac.cn](mailto:hli@dicp.ac.cn). Fax: +86-411-84379517.

### Notes

The authors declare no competing financial interest.

## ACKNOWLEDGMENTS

This work is supported by NSFC of China (Grants 21077101 and 21177124).

## REFERENCES

- (1) Cundill, J. P. *A Dictionary of Explosives*; The Royal Engineers Institute: Chatham, U.K., 1889.
- (2) Turcotte, R.; Fouchard, R. C.; Turcotte, A. M.; Jones, D. E. G. *J. Therm. Anal. Calorim.* **2003**, *73*, 105–118.
- (3) Kapur, G. B.; Hutson, H. R.; Davis, M. A.; Rice, P. L. *J. Trauma-Injury Infect. Crit. Care* **2005**, *59*, 1436–1444.
- (4) Ewing, R. G.; Atkinson, D. A.; Eiceman, G. A.; Ewing, G. J. *Talanta* **2001**, *54*, S15–S29.
- (5) Eiceman, G. A.; Stone, J. A. *Anal. Chem.* **2004**, *76*, 390A–397A.
- (6) Tabrizchi, M.; Ilbeigi, V. *J. Hazard. Mater.* **2010**, *176*, 692–696.
- (7) Fetterolf, D. D.; Clark, T. D. *J. Forensic Sci.* **1993**, *38*, 28–39.
- (8) McGann, W. J.; Haigh, P.; Neves, J. L. *Int. J. Ion Mobil. Spec.* **2002**, *5*, 119–122.
- (9) Crawford, C. L.; Boudries, H.; Reda, R. J.; Roscioli, K. M.; Kaplan, K. A.; Siems, W. F.; Hill, H. H. *Anal. Chem.* **2010**, *82*, 387–393.
- (10) Puton, J.; Nousiainen, M.; Sillanpaa, M. *Talanta* **2008**, *76*, 978–987.
- (11) Daum, K. A.; Atkinson, D. A.; Ewing, R. G. *Talanta* **2001**, *55*, 491–500.
- (12) <http://webbook.nist.gov/chemistry/>.
- (13) Davis, E. J.; Grows, K. F.; Siems, W. F.; Hill, H. H. *Anal. Chem.* **2012**, *84*, 4858–4865.
- (14) Hearley, A. K.; Johnson, B. F. G.; McIndoe, J. S.; Tuck, D. G. *Inorg. Chim. Acta* **2002**, *334*, 105–112.
- (15) Jones, R. O.; Ballone, P. *J. Chem. Phys.* **2003**, *118*, 9257–9265.
- (16) Biermann, R.; Winter, C.; Egelstaff, P. A. *J. Non-Cryst. Solids* **1998**, *309*, 232–234.
- (17) Kozole, J.; Stairs, J. R.; Cho, I.; Harper, J. D.; Lukow, S. R.; Lareau, R. T.; DeBono, R.; Kuja, F. *Anal. Chem.* **2011**, *83*, 8596–8603.
- (18) Kozole, J.; Tomlinson-Phillips, J.; Stairs, J. R.; Harper, J. D.; Lukow, S. R.; Lareau, R. T.; Boudries, H.; Lai, H.; Brauer, C. S. *Talanta* **2012**, *99*, 799–810.